Lab report for CE2164 experiment C1

Lab session on March, 23 2009

Mohanadas Harish Chandar U067314J

April 2, 2009

1 Objectives

The objective of the experiment was to demonstrate the behaviour of concrete beams when subject to bending moments and shear forces, with respect to cracking, deflection, strength, and ductility.

2 Test specimens

Beam B5b was tested. The results obtained were then compared with results from beam B8b, which was tested by another group.

3 Results

3.1 Curves from data acquisition system output

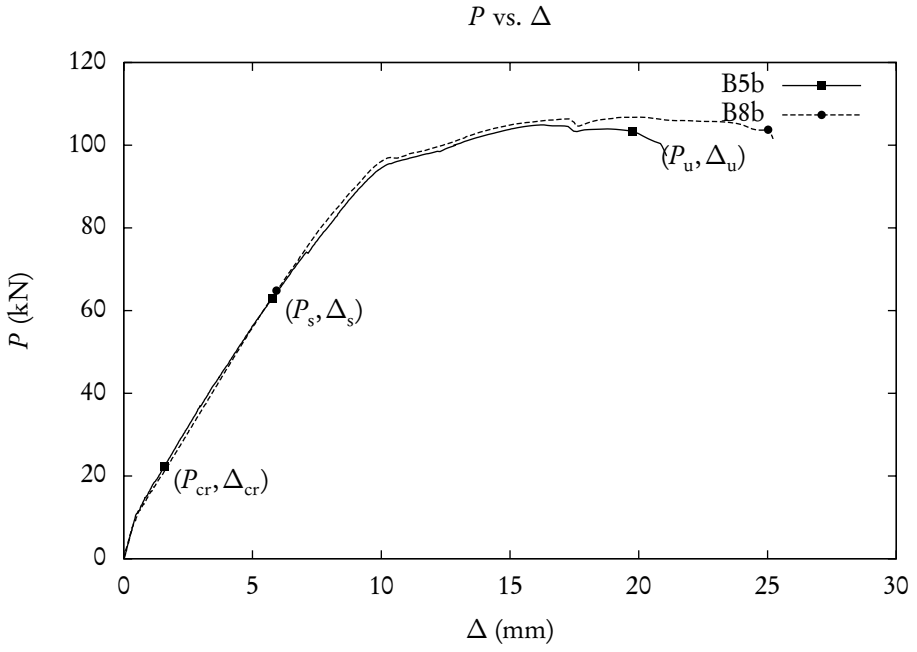

Figure 1: Plot of P vs. Δ for beams B5b and B8b.

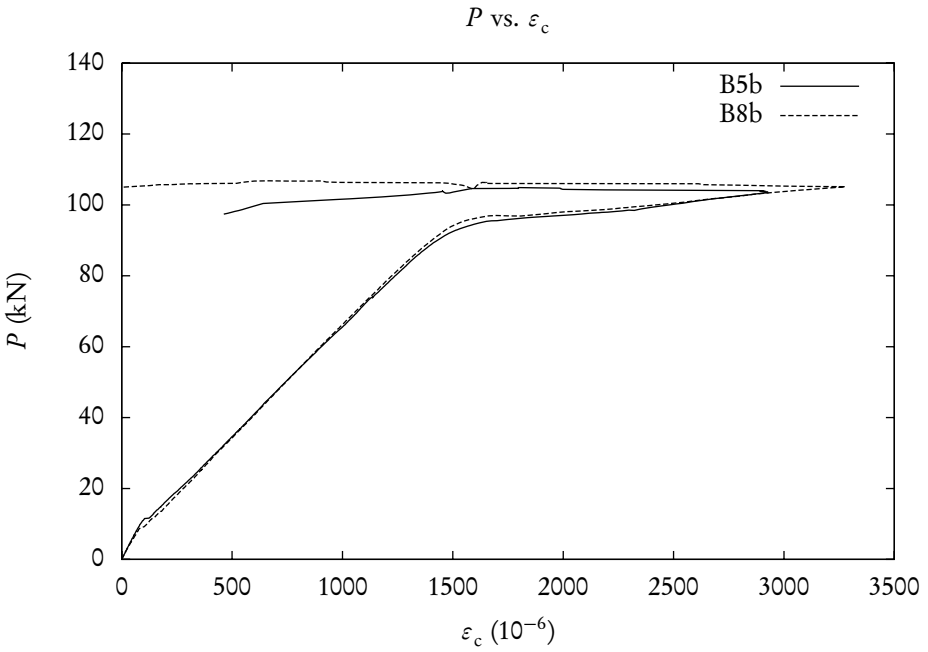

Figure 2: Plot of P vs. ε_c for beams B5b and B8b.

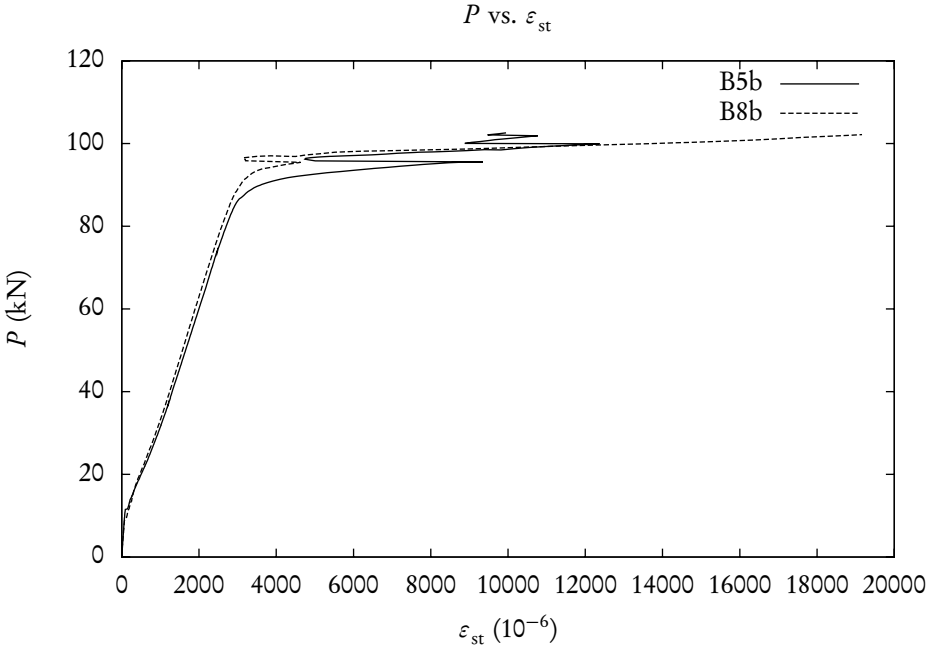

Figure 3: Plot of P vs. ε_{st} for beams B5b and B8b.

3.2 Moment vs. curvature curves

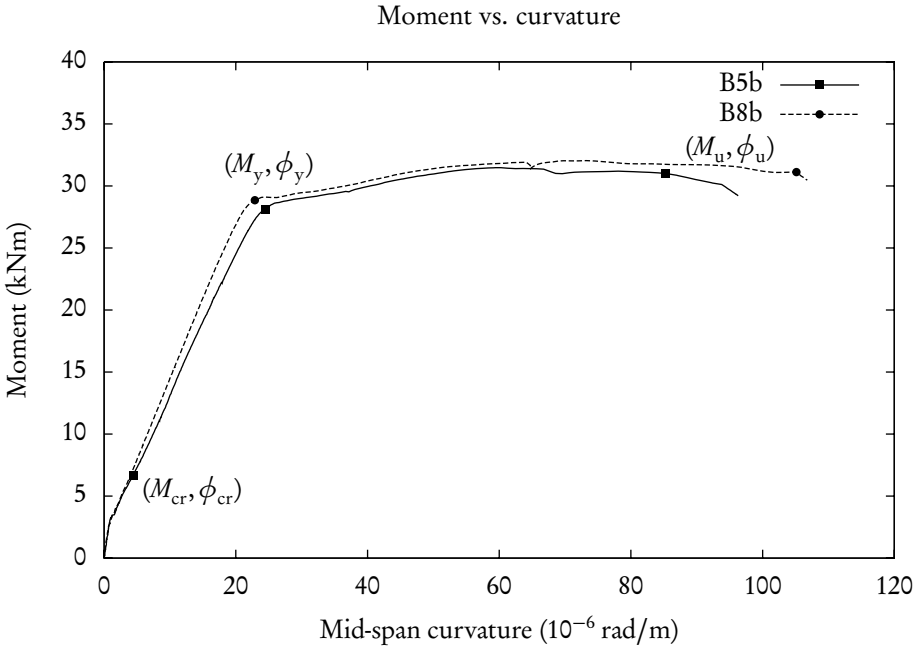

Figure 4: Plot of moment vs. curvature for beams B5b and B8b.

3.3 P vs. crack width

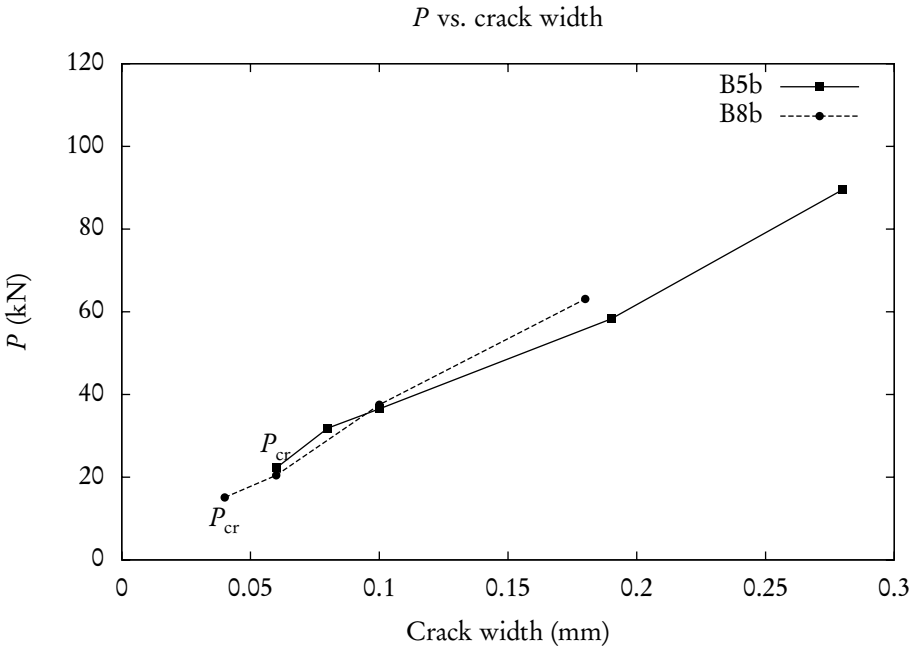

Figure 5: Plot of P vs. crack width for beams B5b and B8b.

3.4 Failure patterns

3.4.1 Beam B5b

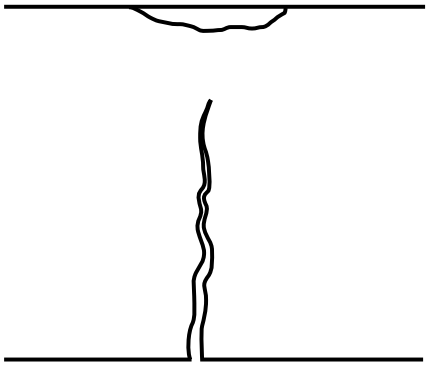

Figure 6: Sketch of failure pattern for beam B5b. Beam B5b failed in flexure.

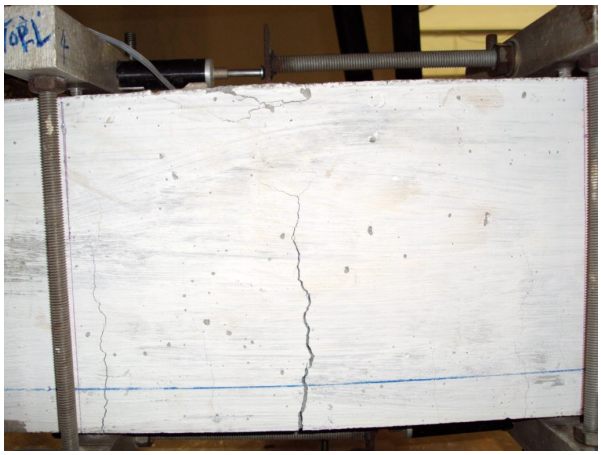

Figure 7: Photograph of the failure pattern for beam B5b.

Figure 8: Photograph of shear cracks for beam B5b. Shear cracks were minimal and thus not recorded.

3.4.2 Beam B8b

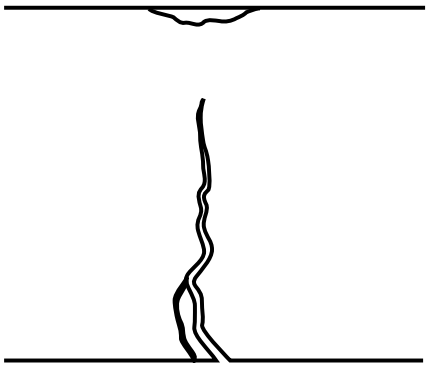

Figure 9: Sketch of failure pattern for beam B8b. Beam B8b failed in flexure.

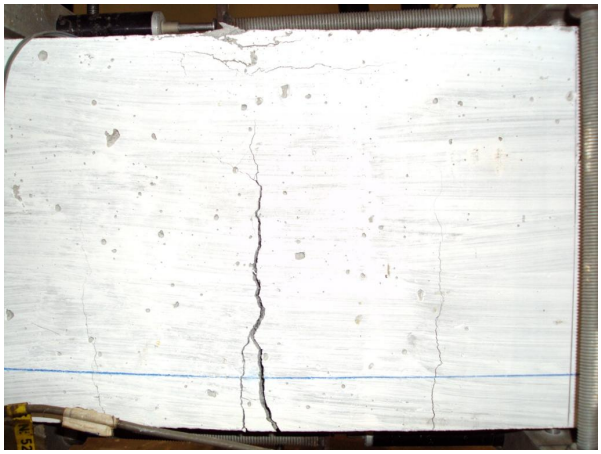

Figure 10: Photograph of failure pattern for beam B8b.

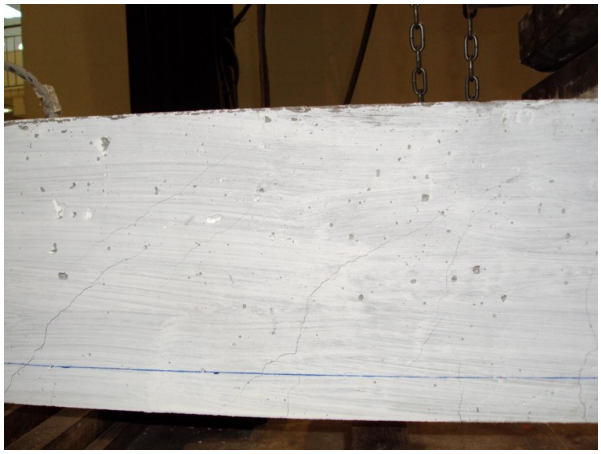

Figure 11: Photograph of shear cracks for beam B8b. Shear cracks were minimal and thus not recorded.

3.5 Strain profiles and curvatures for beam B5b

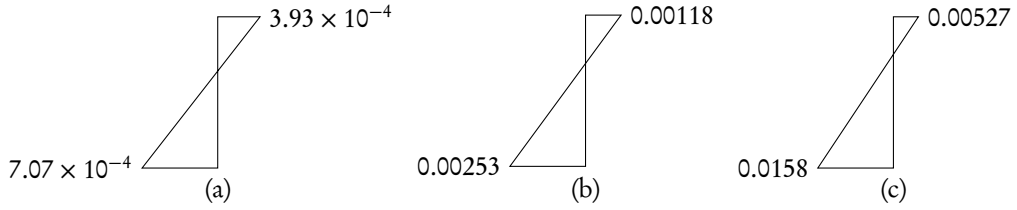

Figure 12: Strain profiles for beam B5b, obtained from curvature meter at (a) just prior to cracking, (b) at the calculated service load, P_s, and (c) near the ultimate load.

3.5.1 Curvature just prior to cracking

$$\begin{aligned}\phi_{cr} &= \frac{\text{top strain} + \text{bottom strain}}{250} \times 10^6 \\ &= \frac{3.94 \times 10^{-4} + 7.07 \times 10^{-4}}{250} \times 10^6 \\ &= 4.40\,\text{rad/m}\end{aligned}$$

3.5.2 Curvature at calculated service load

$$\begin{aligned}\phi_s &= \frac{\text{top strain} + \text{bottom strain}}{250} \times 10^6 \\ &= \frac{0.00118 + 0.00253}{250} \times 10^6 \\ &= 14.85\,\text{rad/m}\end{aligned}$$

3.5.3 Curvature near the ultimate load

$$\begin{aligned}\phi_u &= \frac{\text{top strain} + \text{bottom strain}}{250} \times 10^6 \\ &= \frac{0.00527 + 0.158}{250} \times 10^6 \\ &= 85.33\,\text{rad/m}\end{aligned}$$

3.6 Comparison of test results and theoretical values for beam B5b

Loading stage		Theory	Experimental	Experimental/Theory
At cracking	P_{cr} (kN)	9.00	22.2	2.47
	Δ_{cr} (mm)		0.06	
	f_{st} (N/mm^2)	14.4	122.3	8.49
	f_{cc} (N/mm^2)	2.71	7.22	2.67
At calculated service load	P_s (kN)	50.3	63.01	1.25
	Δ_s (mm)		5.77	
	f_{st} (N/mm^2)	254	400	1.57
	f_{cc} (N/mm^2)	20.2	10.7	0.53
At collapse	P_u (kN)	80.5	100.82	1.25
	Δ_u (mm)		20.65	
	f_{st} (N/mm^2)	400	400	1
	ε_{cu}	0.0035	0.002192	0.63

Table 1: Comparison of test results with theory for beam B5b.

3.6.1 Theoretical calculations at cracking

$$\begin{aligned} A'_s &= 2 \times \pi r^2 \\ &= 2 \times \pi \times 5^2 \\ &= 157.08\,\text{mm}^2 \end{aligned} \qquad \begin{aligned} A_s &= 2 \times \pi r^2 \\ &= 2 \times \pi^2 \\ &= 402.12\,\text{mm}^2 \end{aligned}$$

$$\begin{aligned} \alpha_e &= \frac{200}{24.0} \\ &= 8.333 \end{aligned} \qquad \begin{aligned} (\alpha_e - 1)A'_s &= 1152\,\text{mm}^2 \\ (\alpha_e - 1)A_s &= 2949\,\text{mm}^2 \end{aligned}$$

$$\begin{aligned} x &= \frac{\sum Ax}{\sum A} \\ &= \frac{(200 \times 125)(100) + 1152(26) + 2949(171)}{(200 \times 125) + 1152 + 2949} \\ &= 104.27\,\text{mm} \end{aligned}$$

$$\begin{aligned} I &= \frac{125 \times 200^3}{12} + 125 \times 200 \times (104.27 - 100)^2 + 1152 \times (104.27 - 26)^2 + 2949 \times (171 - 104.27)^2 \\ &= 104.0 \times 10^6\,\text{mm}^4 \end{aligned}$$

$$\text{Thus, } M_{cr} = \frac{f_t/\gamma_m \times I}{y_b} = \frac{3.73/1.5 \times 104.0 \times 10^6}{200 - 104.27} \times 10^{-6} = 2.70\,\text{kNm}$$

$$\text{And } P_{cr} = \frac{M_{cr}}{0.6} \times 2 = \frac{2.70}{0.6} \times 2 = 9.00\,\text{kN}$$

$$f_{cc} = \frac{M_{cr} y_c}{I} = \frac{2.70 \times 10^6 \times 104.27}{104.0 \times 10^6} = 2.71\,\text{N/mm}^2$$

$$f_{st} = \alpha_e \frac{M_{cr} y_{st}}{I} = 8.333 \frac{2.70 \times 10^6 \times (171 - 104.27)}{104.0 \times 10^6} = 14.4\,\text{N/mm}^2$$

3.6.2 Theoretical calculations at collapse

$$\varepsilon_y = \frac{460}{200000} = 0.002 \qquad \varepsilon_{cu} = 0.0035 \qquad f_{cu} = 55.07\,\text{kN/mm}^2$$

Try $x = 100\,\text{mm}$,

$$\varepsilon_{sc} = 0.0035 \frac{d' - x}{x} = 0.0035 \frac{24 - 100}{100} = -0.002660 \text{ Yielded in compression}$$

$$\varepsilon_{st} = 0.0035 \frac{d - x}{x} = 0.0035 \frac{171 - 100}{100} = 0.002485 \text{ Yielded in tension}$$

$$T = A_s f_y/\gamma_m = 402.12 \times 460/1.15 = 160.85\,\text{kN}$$

$$C = C_c + C_s = 0.45 f_{cu} \times b \times 0.9x + A_s' \times f_y/\gamma_m = 0.45 \times 55.07 \times 125 \times 0.9 \times 100 + 157.08 \times 460/1.15 = 341.62\,\text{kN} > T$$

Neutral axis depth needs to be reduced.

After several tries, assume $x = 42.25\,\text{mm}$,

$$\varepsilon_{sc} = 0.0035\frac{d' - x}{x} = 0.0035\frac{24 - 42.25}{42.25} = -0.001346 \text{ Yet to reach yielding}$$

$$\varepsilon_{st} = 0.0035\frac{d - x}{x} = 0.0035\frac{171 - 42.25}{42.25} = 0.01067 \text{ Yielded in tension}$$

$$T = A_s f_y/\gamma_m = 402.12 \times 460/1.15 = 160.9\,\text{kN}$$

$$C = C_c + C_s = 0.45 f_{cu} \times b \times 0.9x + A'_s \times \varepsilon_{sc} \times E_s = 0.45 \times 55.07 \times 125 \times 0.9 \times 100 + 157.08 \times 0.001346 \times 200000 = 160.1\,\text{kN} \simeq T$$

Taking moments about the line of action C_c,

$$M_u = T(d - 0.45x) + C_s(0.45x - d') = 160.9(171 - 0.45 \times 42.25) + 42.29(0.45 \times 45.25 - 26) = 24.15\,\text{kNm}$$

$$P_u = \frac{M_u}{0.6} \times 2 = \frac{24.15}{0.6} \times 2 = 80.5\,\text{kN}$$

$$\varepsilon_{cu} = 0.0035$$

$$f_{st} = \frac{p_y}{\gamma_m} = \frac{460}{1.15} = 400\,\text{N/mm}^2$$

3.6.3 Theoretical calculations at calculated service load

$$P_s = P_u/1.6 = 80.5/1.6 = 50.3\,\text{kN}$$

Using the idealised parabolic stress-strain curve for concrete,

$$f_c = 18571 \times 10^3 {\varepsilon_c}^2 + 33.33\varepsilon_c$$

The maximum ε_c to which this applies is

$$2.4 \times 10^{-4} \sqrt{f_{cu}/\gamma_m} = 2.4 \times 10^{-4} \sqrt{55.07/1.5} = 0.001454$$

Taking H to be the distance vertically upwards from neutral axis and $\bar{H}$ to be the vertical axis centroid of C_c,

$$\bar{H} = \frac{\int_0^x H f_c \, dH}{\int_0^x f_c \, dH}$$

Depth from top of beam to vertical centroid of C_c, $d_c = x - \bar{H}$.

After several attempts using a spreadsheet, assume $\varepsilon_{cc} = 0.001311 < 0.001454$ and $x = 86.93$ mm,

$\varepsilon_{sc} = 9.19 \times 10^3$ Yet to reach yielding	$\varepsilon_{st} = 0.001268$ Yet to reach yielding
$T = 101.9\,\text{kN}$	$C = 101.9\,\text{kN} \simeq T$
$\bar{H} = 65.15\,\text{mm}$	$d_c = 21.78\,\text{mm}$
$M_s = 15.09\,\text{kNm}$	$P_s = 50.3\,\text{kN} = P_s\text{wanted}$
$f_{cc} = 20.1\,\text{N/mm}^2$	$f_{st} = 254\,\text{N/mm}^2$

4 Discussion

4.1 Descriptions

4.1.1 Beam behaviour and type of failures for beam B5b and beam B8b

Beam B5b failed in flexure at an ultimate load of 100.8 kN. Flexural cracks were first observed at a load of 22.2 kN at the bottom of the beam within the flexural zone. At increading loads, a single large flexural crack propagated vertically upwards from the midspan. Shear cracks were minimal and were thus not recorded.

Beam B8b failed in flexure at an ultimate load of 103.7 kN. Flexural cracks were first observed at a load of 15.1 kN at the bottom of the beam within the flexural zone. At increading loads, a large flexural crack, located slightly to the right of the midspan, propagated upwards. A smaller crack, located slightly to the left of the midspan, also propagated upwards and joined the abovementioned large flexural crack. Shear cracks were minimal and were thus not recorded.

4.1.2 Load-deflection

Beam B5b had an initial linear load-deflection relationship (Figure 1) up to about 10 kN. From 10 kN to about 90 kN, the relationship was still fairly linear, although the gradient of the load-deflection curve had markedly reduced. Beyond 90 kN, the load remained fairly constant for another 10 mm of deflection. An ultimate load of 100.8 kN was reached before unloading began.

4.1.3 Moment-curvature

Beam B5b had an initial linear moment-curvature relationship (Figure 4) up to about 3 kNm. From 3 kNm to about 28 kNm, the relationship was still fairly linear, although the gradient of the curve had markedly reduced. Beyond 28 kNm, the moment remained fairly constant with the curvature increasing from about 24.5 rad/m to about 92 rad/m.

4.1.4 Load-compressive concrete strain

The initial load-compressive strain relationship (Figure 2) for beam B5b was fairly linear to about 90 kN. From 90 kN and to about 100 kN, the relationship was again fairly linear but with a greatly reduced gradient. Beyond a certain deflection of the beam within the ductile region, the concrete strain started to decrease considerably, probably due to cracking of concrete at the top of the beam.

4.1.5 Load-tensile steel strain

The initial load-tensile steel strain relationship (Figure 3) for beam B5b was fairly linear to about 85 kN. From 85 kN and to about 90 kN, the relationship was again fairly linear but with a greatly reduced gradient. Beyond 90 kN, the load-tensile steel strain relationship was erratic, suggesting that there was slipping of concrete past the steel bars due to sudden expansion of cracks.

4.1.6 Strain profile

The strain profiles for beam B5b, obtained from the curvature meter, are given in Figure 12). It was observed that the depth of the neutral axis decreases with increased loading. At near the ultimate load, the strain profiles obtained from the curvature meter disagree with the strain gauge readings at the top of the beam and at the tensile steel reinforcement. This is probably due to cracking of concrete at the top of the beam, slipping of concrete past the tensile steel reinforcement, or failure of the strain gauges.

4.2 Comparisons between beam B5b and beam B8b

4.2.1 Load-deflection curves

Beam B8b had a similar initial piecewise linear load-deflection relationship as Beam B5b (Figure 1). The second linear region was however slightly larger, ranging from 10 kN to 95 kN. Beyond 90 kN the load remained fairly constant over a significantly larger deflection range of 16 mm. It is likely that the reduced spacing between shear links significantly contributed to this effect.

4.2.2 Moment-curvature curves

Beam B8b had a similar initial piecewise linear moment-curvature relationship as Beam B5b (Figure 4). The gradient of the second linear region was however slightly larger. The ductile region of beam B8b was however considerably larger than that of beam B5b. It is likely that the reduced spacing between shear links significantly contributed to this increase in ductility.

4.2.3 Load-crack width curves

The load-crack width relationship (Figure 5) for the two beams were fairly similar. The recorded P_{cr} for beam B8b was lower than that for beam B5b. However, no record for a crack width of 0.04 mm was made for beam B5b. Moreover, the loads at a crack width of 0.06 mm for both beams were greatly similar. Thus, the difference in recorded P_{cr} is likely due to better observation during the test for beam B8b rather than any inherent differences between the beams.

4.2.4 Crack patterns

The crack patterns of both beams were fairly similar. There was a slight difference in the crack propagation as beam B5b had one single large crack at midspan while beam B8b had one large crack and one smaller one

that began to the right and left of the midspan respectively (Figures 9 and 10). This slight difference is however attributed to random effects.

The load-tensile steel strain curve (Figure 3) for beam B8b is much more stable that that of beam B5b at loads beyond 90 kN. This suggests that near the ultimate load, the expansion of cracks in beam B8b occurred more smoothly than in beam B5b. The closer spacing between shear links in beam B5b is likely to have significantly contributed to this effect.

4.2.5 Ultimate loads

The ultimate loads of both beams were greatly similar (Figure 1). This shows that given sufficient shear reinforcement, shear link spacing has negligible effect on ultimate load.

4.2.6 Failure modes

Both beams failed in flexure in a similar manner (Figures 6, 7, 6, 7) at similar ultimate loads. However, Figure 2 shows that the maximum concrete strain at top of beam attained before cracking was greater in beam B8b than in beam B5b. This improved concrete stability in beam B8b may be due to its reduced spacing between shear links.

4.3 Comparison of test results and theoretical values for beam B5b

A comparison of test results and theoretical values are given in Table 1. As expected, the theoretical values for service load ultimate load were lower than their respective experimental values due to inclusion of partial safety factors and conservative design idealisations.

The experimental values for cracking load seems unusually high since it is about 2.5 times the theoretical cracking load. This discrepency is probably due to late observation of flexural crack initiation. Late observation of flexural crack initiation can also be used to explain the unusually high values for average tensile steel stress at flexural zone, f_{st}, and for concrete stress at top of beam at flexural zone, f_{cc}.

The theoretical value for f_{cc} at calculated service load is only about half its corresponding experiemental value. This shows that the parabolic-rectangular idealised stress-strain curve for concrete is conservative, even after accounting for the partial safety factor of concrete.

At failure, the ultimate compressive strain at the top of the beam, ε_{cu} was much lower than the theoretical failure strain of concrete. This discrepency is likely due to cracking of concrete at the top of the beam, which lead to severely reduced concrete strain gauge values.

5 Conclusion

The main difference between the test specimens was the closer spacing between shear links in beam B5b as compared to beam B8b. The experiment showed that both beams were designed to be under-reinforced and fail in flexure. The shear reinforcement in both beams was sufficient.

Beam B8b had a greater ductility, greater deflection capacity and better cracking stability than beam B5b. On the other hand, both beams had similar ultimate ultimate loads. This showed that given sufficient shear reinforcement, a closer shear link spacing increases ductility, deflection capacity and cracking stability but has negligible effect on beam strength.